

SIRI-Bench: Challenging VLMs’ Spatial Intelligence through Complex Reasoning Tasks

Zijian Song¹, Xiaoxin Lin¹, Qiuming Huang¹, Guangrun Wang^{1*}, Liang Lin¹

¹Sun Yat-sen University,

{songzj8, linxx76, huangqm}@mail2.sysu.edu.cn,
wanggrun@gmail.com, linliang@ieee.org

Abstract

Large Language Models (LLMs) are experiencing rapid advancements in complex reasoning, exhibiting remarkable generalization in mathematics and programming. In contrast, while spatial intelligence is fundamental for Vision-Language Models (VLMs) in real-world interaction, the systematic evaluation of their complex reasoning ability within spatial contexts remains underexplored. To bridge this gap, we introduce SIRI-Bench, a benchmark designed to evaluate VLMs’ spatial intelligence through video-based reasoning tasks. SIRI-Bench comprises nearly 1K video-question-answer triplets, where each problem is embedded in a realistic 3D scene and captured by video. By carefully designing questions and corresponding 3D scenes, our benchmark ensures that solving the questions requires both spatial comprehension for extracting information and high-level reasoning for deriving solutions, making it a challenging benchmark for evaluating VLMs. To facilitate large-scale data synthesis, we develop an Automatic Scene Creation Engine. This engine, leveraging multiple specialized LLM agents, can generate realistic 3D scenes from abstract math problems, ensuring faithfulness to the original descriptions. Experimental results reveal that state-of-the-art VLMs struggle significantly on SIRI-Bench, underscoring the challenge of spatial reasoning. We hope that our study will bring researchers’ attention to spatially grounded reasoning and advance VLMs in visual problem-solving.

1 Introduction

Recent advancements in Large Language Models (LLMs) and Vision-Language Models (VLMs) have significantly enhanced their complex reasoning capability, demonstrating remarkable problem-solving proficiency (Wei et al., 2022; Lu et al.,

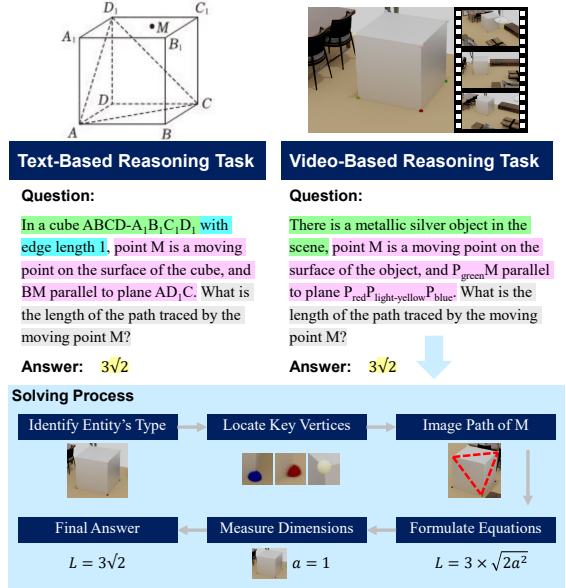


Figure 1: **Complex Reasoning in Visual Domain.** Conventional benchmarks typically involve complex reasoning tasks in text format (left col.), where reasoning occurs entirely within language modality. In contrast, this work introduces video-based reasoning tasks (right col.), where key conditions are implicitly embedded in realistic 3D scenes and captured as videos. Solving these problems requires interleaved textual reasoning and spatial perception (bottom row), evaluating VLMs’ reasoning ability grounded in spatial comprehension.

2025; Fan et al., 2025; Jaech et al., 2024; Guo et al., 2025). By leveraging extensive training on math problem solving and programming, these models have demonstrated extraordinary generalization across diverse, intricate challenges (Lewkowycz et al., 2022; Achiam et al., 2023; Chen et al., 2024b; Saab et al., 2024; Chen et al., 2024c, 2021b; Li et al., 2022).

With the increasing focus on complex problem solving, various benchmarks have been developed to evaluate the reasoning ability of LLMs and VLMs (Hendrycks et al., 2021; Johnson et al.,

*Corresponding author.

2017; Goyal et al., 2017; Hudson and Manning, 2019; Liu et al., 2024; Chen et al., 2024e; Fu et al., 2024). However, existing studies predominantly focus on abstract problems, such as algebraic computation, program synthesis, and geometric reasoning (Lu et al., 2023; Wang et al., 2024a; Chen et al., 2021a; Zhang et al., 2024a; Amini et al., 2019; Zhang et al., 2024b), largely overlooking visual-based reasoning tasks that are crucial for real-world interaction. Among these, spatial intelligence remains particularly underexplored.

Spatial intelligence refers to the ability to reason about spatial information (Gardner, 2011); it requires myriad capabilities, including perceiving size and shape, understanding geometric transformations, and retrieving spatial knowledge (Yang et al., 2024b). This capability is essential not only for the VLMs themselves but also for downstream real-world applications (Chen et al., 2024a), such as robotics (Brohan et al., 2023, 2022; O’Neill et al., 2024), augmented reality (Mangalam et al., 2023; Grauman et al., 2022; Chandrasegaran et al., 2024; Yuan et al., 2024b, 2025c), and embodied AI (Driess et al., 2023; Liu et al., 2025). While some notable studies have explored spatial intelligence (Yang et al., 2024b; Team, 2024e,a; Zhai et al., 2025; Li et al., 2024; Man et al., 2024), many of them remain centered on perception tasks, such as scene understanding and distance estimation. These tasks are essential, yet they fall short of evaluating the high-level reasoning capability indispensable for spatial problem-solving. Notably, there is still a lack of a systematic framework for evaluating spatially grounded reasoning.

To address this limitation, we introduce the **Spatial Intelligence Reasoning Benchmark (SIRI-Bench)**, specifically designed to evaluate VLMs’ spatial intelligence through complex reasoning tasks. SIRI-Bench consists of 891 samples, with each sample being a video-question-answer triplet. Inspired by the typical paradigm of assessing textual reasoning via math problems (Zhang et al., 2024b; Lu et al., 2023; Wang et al., 2024a; Yue et al., 2024; the University of Utah, 2024; Lightman et al., 2023), we take 3D-geometry math problems as the foundation to construct our benchmark. Unlike conventional textual or 2D diagram-based representations, where problem conditions are explicitly stated in text or diagrams, SIRI-Bench presents these problems through video-based inputs. As shown in the fig. 1, each math problem

in SIRI-Bench is represented as a 3D scene and captured as a video. In this representation, key mathematical conditions and spatial relationships are implicitly embedded within the 3D scene, requiring models to interpret and reason based on spatial cues. More examples can be found in fig. 3. By carefully designing the representation of each question, SIRI-Bench ensures that both spatial perception and high-level reasoning capabilities are essential to successfully solve the questions. Consequently, the SIRI-Bench provides a systematic and challenging benchmark for evaluating VLMs on spatially grounded reasoning tasks, offering new insights into spatial intelligence and visual problem-solving.

Constructing such a dataset at scale entails significant challenges. Manually annotating and crafting the 3D scene is extremely labor-intensive, as it requires expertise in both math and 3D software. To address these challenges, we develop an Automatic Scene Creation Engine that automatically translates a 3D geometry problem into a realistic 3D scene and renders a corresponding video. This engine employs multiple tailored LLM agents and follows a sophisticated workflow. Specifically, the Automatic Scene Creation Engine takes as input a 3D geometry math problem along with its answer. Initially, the engine solves for the type and specific dimensions of the geometric entity. Following this, the corresponding Blender Python (Blender Online Community, 2022) script (bpy script) is generated to insert the geometric entity into the Blender scene. After that, the vertex indices are transformed from letter-based indexing to color-based indexing, providing precise references. Subsequently, the text description of the problem is modified by identifying and removing the information that can be inferred from the scene. This prevents the model being tested from bypassing spatial interpretation and directly relying on text. Finally, the video of the geometric entity as well as the whole scene is captured, which will serve as the visual input for VLMs. We show samples in fig. 3, which verify that the proposed Automatic Scene Creation Engine is capable of accepting any 3D geometry math problem and generating the corresponding 3D scene faithful to the original description.

We conduct extensive experiments on SIRI-Bench, evaluating various popular VLMs. Results show that over 50% of the problems in SIRI-Bench cannot be correctly solved even by the most state-

of-the-art VLMs, with prediction errors exceeding 100% compared to the ground truth. Remarkably, when key mathematical conditions, such as object dimensions and geometric types, are explicitly provided in textual format, the models’ performance improves by more than twofold. This indicates that VLMs struggle to extract the necessary spatial information from video. In addition, comparisons with human participants and qualitative visualizations also show that current VLMs fail to solve SIRI-Bench problems accurately. These findings reveal certain limitations of existing VLMs in spatially grounded reasoning and highlight the value of SIRI-Bench.

The major contributions of this paper are summarized as follows:

(1) We introduce the SIRI-Bench, a benchmark designed to investigate VLMs’ spatial intelligence through complex reasoning tasks. By representing problems through video-based 3D scenes, SIRI-Bench establishes a novel framework for evaluating VLMs’ reasoning capability grounded in spatial comprehension.

(2) We develop an Automatic Scene Creation Engine that transforms 3D geometry problems into realistic 3D scenes. By leveraging multiple specialized LLM agents in a structured workflow, the engine can produce faithful 3D scenes and significantly reduce the cost of large-scale data generation.

(3) We benchmark the performance of state-of-the-art VLMs on SIRI-Bench, and find that they struggle to extract critical spatial information from visual inputs when solving complex reasoning tasks, revealing key limitations in spatially grounded reasoning.

2 Related Work

2.1 Spatial intelligence

Spatial intelligence is a key aspect of cognitive functioning and has increasingly garnered attention within Vision-Language Models. The concept of ‘Spatial AI’ was introduced by Davison et al. (Davison, 2018), which is defined as an extension of visual SLAM (Simultaneous Localization and Mapping). Following this, Chen et al. (Chen et al., 2024a) presented SpatialVLM, a VLM trained on a 3D visual question answering dataset, which demonstrated significant improvements in spatial dimension estimation. Yang et al. (Yang et al., 2024b) further formalized the visual-spatial intel-

ligence as the capability to understand, interpret, and operate visual information in 3D space. These studies highlight the importance of spatial intelligence in robotics and autonomous systems. In addition to 3D understanding (Yuan et al., 2025a,b, 2024a; Chen et al., 2024d; Mao et al., 2025), spatial generation is another key component of spatial intelligence. The team of Li et al. developed the World Labs system (Team, 2024e), which generates interactive 3D scenes from a single image, demonstrating the generative potential of spatial intelligence. Similarly, the DeepMind team released the Genie 2 (Team, 2024a), which supports physical simulation and spatial memory capabilities. While existing VLMs excel at elementary tasks, this paper seeks to advance the field by investigating the more intricate challenges of complex spatial reasoning.

2.2 Complex Reasoning

Complex reasoning refers to the capability of language models to generate logically consistent and contextually appropriate responses through multi-step reasoning, abstract thinking, and knowledge integration. Researches have shown that LLMs possess the capability to handle complex logical reasoning (Wei et al., 2022; Lu et al., 2025; Fan et al., 2025). This technology has been widely applied across various domains, including mathematical problem-solving (Lewkowycz et al., 2022; Hendrycks et al., 2021; Achiam et al., 2023; Jaech et al., 2024; Guo et al., 2025), medical diagnosis (Chen et al., 2024b; Saab et al., 2024; Chen et al., 2024c), and programming (Chen et al., 2021b; Li et al., 2022; Jaech et al., 2024; Guo et al., 2025), etc. However, researchers found that LLMs struggle with visual-language reasoning. This may be due to their inherent inability to process and integrate visual-linguistic information, limiting their real-world applications like robotics (Małkiński et al., 2024; Chia et al., 2024; Ghosal et al., 2024). Although VLMs achieve proficiency in conventional video question-answering tasks involving recognition and description (Wang et al., 2024b; Team, 2024b; Lin et al., 2023; Maaz et al., 2023), their capacity for integrating complex reasoning with spatial intelligence remains underdeveloped. To address this limitation, this paper represents math problems through video-based 3D scenes that jointly demand both spatial understanding and high-level reasoning.

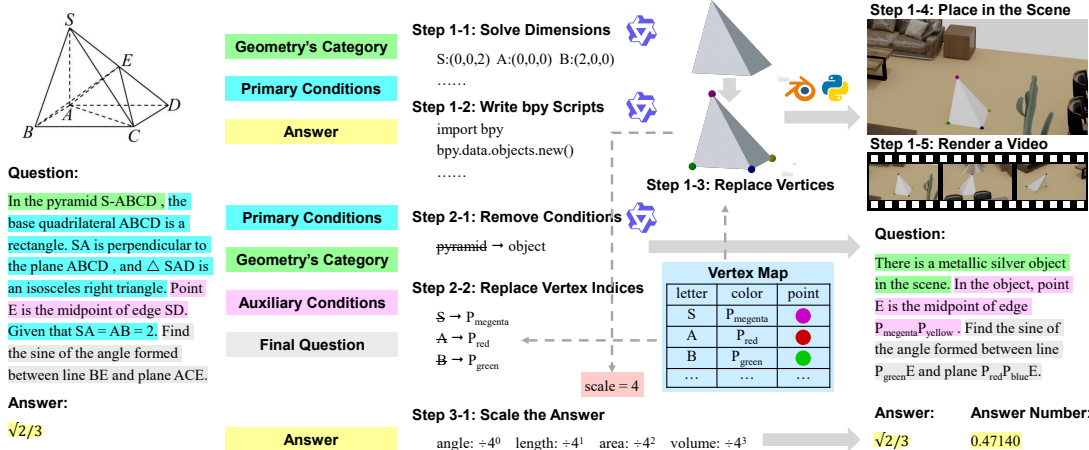


Figure 2: **Illustration of the Transformation Process** from a raw math problem to a 3D Spatial Representation. The given math problem is decomposed into five components and processed individually. First, the specific dimensions of the main geometric entity are solved, and corresponding bpy code is generated to insert the entity into a 3D scene, which is then captured as a video. Next, the problem conditions are filtered to remove information that must be inferred from the 3D space rather than the text, and node indices are replaced. Finally, the answer is adjusted for scaling effects to produce the final answer.

2.3 VLM Reasoning Benchmark

Recent advances in VLMs have spurred the development of diverse evaluation benchmarks designed to rigorously test various aspects of visual reasoning. Some benchmarks focus on evaluating the visual reasoning capability of VLMs by minimizing linguistic biases and ensuring reliance on authentic visual input (Johnson et al., 2017; Goyal et al., 2017; Hudson and Manning, 2019; Liu et al., 2024; Chen et al., 2024e; Fu et al., 2024). Benchmarks such as MathVista (Lu et al., 2023), MATH-Vision (Wang et al., 2024a), GeoQA (Chen et al., 2021a), Geoeval (Zhang et al., 2024a), Mathqa (Amini et al., 2019) and MathVerse (Zhang et al., 2024b) primarily assess the symbolic and geometric reasoning of VLM through plane geometry problems, yet remain abstracted from real-world contexts, limiting their capacity to evaluate spatially grounded understanding. Unlike existing 2D-centric VLM benchmarks, our benchmark is built upon realistic 3D environments with precise geometric properties (e.g., angles, distances). Furthermore, to rigorously evaluate VLMs’ complex spatial reasoning, our benchmark demands multi-step logical inference that integrates spatial perception with procedural reasoning.

3 SIRI-Bench

To evaluate the spatial intelligence of VLMs in complex reasoning scenarios, we introduce SIRI-

Bench, a benchmark that centers on both spatial awareness and complex mathematical reasoning. The instances in SIRI-Bench are derived from 3D geometry math problems and are transformed into video-based question answering problems. For each problem, we elaborately design the 3D spatial representation that embeds key mathematical conditions into realistic 3D scenes, requiring VLMs to extract relevant information through spatial perception and reasoning.

In this section, we introduce the data collection process, the 3D spatial representation as well as the Automatic Scene Creation Engine for our SIRI-Bench. Additionally, we present other details, some illustrative samples, and data statistics at the end of this section. The processing pipeline for each sample in our dataset is illustrated in fig. 2. And samples from SIRI-Bench as well as the corresponding intermediate steps are shown in fig. 2.

Note that in this paper, the term ‘3D spatial representation’ refers to representing math problems as 3D scenes, in contrast to the text-based or diagram-based representations. It should not be confused with learnable 3D representations or learnable parameters such as those used in 3D Gaussian splatting.

3.1 Data Collection

Following prior works that adopt math problems for complex reasoning (Zhang et al., 2024b; Lu et al., 2023; Wang et al., 2024a; Yue et al., 2024; the

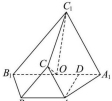
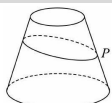
Original Questions	Intermediate Steps	Final Samples
<p>ID: 0008</p>  <p>Question: Given a frustum of a triangular pyramid $ABC-A_1B_1C_1$, where $AB = BC = CA = AA_1 = BB_1 = 2$ and $AA_1 \perp BC$. Point O is the midpoint of line segment A_1B_1, and point D is the midpoint of line segment OA_1. Plane BCC_1B_1 is perpendicular to plane ACC_1A_1. Find the size of the angle formed between line AA_1 and plane BCC_1B_1.</p> <p>Answer: $\pi/4$</p>	<p>Dimensions: A: (0, 0, 0) B: (2, 0, 0) C: (1, $\sqrt{3}$, 0) A₁: (-1, $\sqrt{3}/3$, $2\sqrt{6}/3$) B₁: (3, $\sqrt{3}/3$, $2\sqrt{6}/3$) C₁: (1, $7\sqrt{3}/3$, $2\sqrt{6}/3$)</p> <p>Scale: 4</p> 	<p>Question: There is a metallic silver object in the scene. In the object, point O is the midpoint of line segment $P_{\text{light-red}}P_{\text{light-green}}$ and point D is the midpoint of line segment $OP_{\text{light-red}}$. Find the size of the angle formed between line $P_{\text{red}}P_{\text{light-red}}$ and plane $P_{\text{green}}P_{\text{blue}}P_{\text{light-blue}}P_{\text{light-green}}$.</p> <p>Answer Number: 0.785398</p>
<p>ID: 1289</p>  <p>Question: The upper base radius of the frustum of a cone is 1, the lower base radius is 2, and the slant height is 4. Point P is the midpoint of one of the generatrices of the frustum. If a particle starts from point P, moves around the lateral surface of the frustum once, and returns to point P, what is the length of the shortest path taken by the particle?</p> <p>Answer: $6\sqrt{2}$</p>	<p>Dimensions: h: $\sqrt{15}$ r1: 1 r2: 2</p> <p>Scale: 4</p> 	<p>Question: There is a metallic silver object in the scene. In the object, point P is the midpoint of one of the generatrices of the object. If a particle starts from point P, moves around the lateral surface of the silver object once, and returns to point P, what is the length of the shortest path taken by the particle?</p> <p>Answer Number: 2.12132</p>

Figure 3: **Data Samples in SIRI-Bench.** This figure presents several samples from our SIRI-Bench dataset, along with their original questions and intermediate steps in the data generation process. As can be consistently observed across multiple examples, our data generation engine accurately solves for geometric conditions, replaces vertex indices, processes textual conditions, and computes numerical answers, demonstrating its reliability.

University of Utah, 2024; Lightman et al., 2023), we similarly build our benchmark based on math problems. Math problems naturally involve multi-step and structural inference, making them an ideal foundation for our benchmark. The key distinction is that we focus on 3D geometry math problems rather than algebra or plane geometry problems, and transform them into realistic 3D scenes for spatial reasoning.

The SIRI-Bench is initially collected by gathering publicly available 3D geometry math problems as well as their corresponding answers from online educational resources. These problems are then translated into English for consistency. The dataset encompasses a wide range of difficulty levels, spanning from middle school examination standards to those of high school graduation exams. This broad spectrum ensures that our benchmark accommodates varying degrees of complexity. To maintain data quality, we conduct a manual screening to eliminate low-quality problems. The dataset originally comprises various question types, including multiple-choice questions, fill-in-the-blank questions, and open-ended problem-solving questions. As for the proof-based questions, we exclude them due to the substantial challenge of validating the proof texts. We then leverage LLMs to convert all questions into open-ended problem-solving questions. This transformation ensures that the evaluation is conducted within a standardized and consistent open-ended question-answer format.

3.2 3D Spatial Representation

In this section, we propose a 3D spatial representation that presents geometry problems in realistic 3D scenes, which are then recorded as videos. Compared to traditional abstract representations, such as

textual descriptions or 2D diagrams, this representation offers a closer approximation of real-world scenarios. Moreover, by embedding key mathematical information within the 3D scenes, VLMs are compelled to extract information from spatial cues rather than relying on textual descriptions, thereby jointly assessing their spatial and reasoning abilities.

Specifically, an original 3D geometry problem can be conceptually decomposed into five components: (1) the *Illustration Diagram*, (2) the *Geometry’s Category*, (3) the *Primary Conditions*, (4) the *Auxiliary Conditions*, and (5) the *Final Question*.

For the *Illustration Diagram*, it is typically used to visually represent the problem. In our approach, we discard the diagram and represent the problem through a video that depicts a 3D scene.

For the *Geometry’s Category*, it refers to the type of the main geometric entity involved in the problem. In our approach, we remove this information from the textual description and instead place the corresponding geometric entity within the 3D scene. For example, if the original description states “In the pyramid $S-ABCD$ ” we change it to “There is an object in the scene” and insert a cube into the 3D scene. Notably, since 3D geometry problems follows a strict naming convention, the main geometry category can often be inferred from the vertex indices. For example, a quadrangular pyramid can be inferred from ‘ $P-ABCD$ ’. Therefore, the vertex indices relevant to the main geometric entity must be removed. In order to achieve this, we replace the letter-based indices with color-based indices and correspondingly insert colored points in the scene. This ensures that referring to different colored points accurately represents the vertices on the geometric entity. For example, in the fig. 2, the

vertex ‘ S ’ is replaced with the ‘ $P_{megenta}$ ’, referring to the apex of the pyramid.

For the *primary geometric conditions*, they refer to the specific attributes and constraints of the main geometric entity, such as its dimensions, and spatial relationships (e.g., parallelism or perpendicularity). We also remove this information from the textual description and represent it within the 3D scene. Specifically, based on the original mathematical description, we solve for all the necessary information required to uniquely define the main geometric entity. Based on this information, we insert a corresponding 3D object into the scene. This ensures that all relevant conditions can be re-derived by observing the inserted entity.

For the *auxiliary conditions*, these are additional information that are not directly related to the main geometric entity but are necessary for solving the problem. Given their diverse forms and the potential complexity in representing them visually, we retain these conditions in textual form to ensure clarity and accuracy.

For the *final question*, it specifies what ultimately needs to be solved in the problem. We retain this component in textual format since it clearly states the objective.

Our approach is conceptually aligned with MathVerse (Zhang et al., 2024b), which embeds math conditions into 2D diagrams, challenging the visual capability of VLMs. Unlike MathVerse, by encoding key information in 3D scenes rather than static diagrams, we push the problem setting closer to real-world scenarios. This representation goes beyond optical character recognition (OCR), demanding spatial perception and reasoning. As the VLM must actively interpret the 3D space to extract the necessary information for problem-solving.

3.3 Automatic Scene Creation Engine

Manually converting each problem into a 3D scene is extremely labor-intensive, as it requires both solving the math problems and mastering 3D modeling software. To facilitate large-scale 3D scene generation, we develop an Automatic Scene Creation Engine. Inspired by prior works in Multi-Agent System (Wu et al., 2023; Hong et al., 2023; Yu et al., 2025; Wei et al., 2024; Yang et al., 2024c), we leverage multiple specialized LLM agents to collaboratively create 3D scenes. They follow a sophisticated workflow involving geometric solving, bpy script generation, question processing, and

answer processing. This section outlines this workflow in detail.

First, the engine begins by processing the original 3D geometry problem and its associated answer. To resolve the geometric structure described in the problem, an LLM agent first identifies the type of the main geometric entity. Based on this, we employ a math-specialist agent to solve for all key conditions necessary to fully define the main geometric entity. Specifically, we adopt the QwQ-32B model (Team, 2025b) as the math-specialist agent, which is known for its strong performance on math problems (Team, 2025b). Next, we normalize the size of all geometric entities, scaling them to a size range of 0.5m to 2m (excluding 2m), ensuring that each object fits well within a unified camera configuration. The normalized geometric dimensions are then passed to a code-specialist agent, which generates bpy scripts (Blender Online Community, 2022) to automatically insert the defined objects into Blender. Specifically, we adopt the Qwen-LM (Yang et al., 2024a) as the code-specialist agent, which has been shown to robustly synthesize code (Yang et al., 2024a). Additionally, the generated code also involves inserting colored vertices, which replace letter-based indices with color-based indices (see section 3.2).

Second, the problem description is refined to align with the spatial reasoning objective. Specifically, given the original problem descriptions, an LLM agent identifies and removes key geometric conditions that are intended to be inferred from the 3D scene. As discussed in section 3.2, this step ensures that the VLMs being evaluated must rely on spatial comprehension rather than textual cues to extract such information from 3D scenes.

Third, the original answer is also refined to support robust evaluation. An LLM agent converts symbolic expressions into numerical values, allowing minor estimation errors. For example, when compared to the ground-truth answer $\sqrt{2}$, answers with minor deviations, such as 1.414 or 1.4, should not be considered absolutely incorrect. The agent also adjusts the answer to account for the applied geometric scaling: lengths are scaled linearly, areas quadratically, and volumes cubically, depending on the type of quantity.

By elaborately designing the specialized agents and their collaborative workflow, our Automatic Scene Creation Engine is able to take any 3D geometry problem as input and generate a faithful

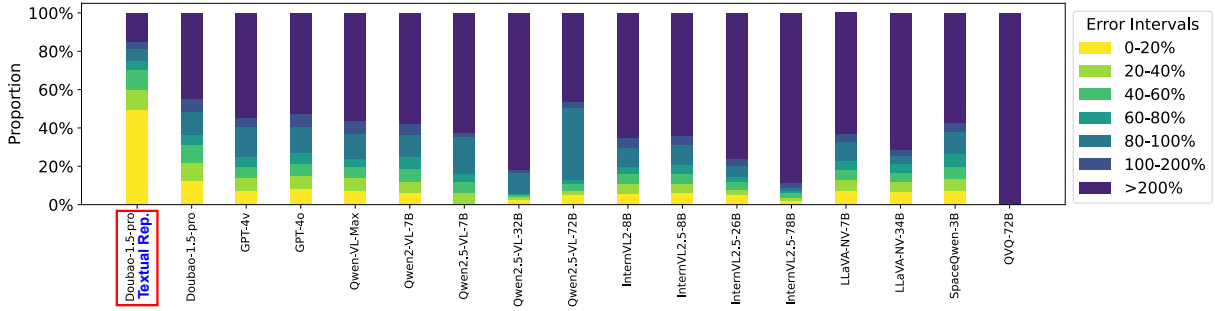


Figure 4: **Overall Performance of Existing VLMs.** This figure shows the error distributions across seven intervals ranging from 0% to 200% for all baseline methods on the SIRI-Bench. Each bar represents a different method, with colors indicating the corresponding error intervals. A higher concentration of errors in the lower intervals (i.e. brighter colors) indicates higher accuracy in problem-solving. The method labeled ‘Textual Rep.’ refers to an LLM that accesses full mathematical conditions through textual descriptions rather than videos of 3D scenes. Overall, the results reveal the limitations of current VLMs in spatially grounded reasoning.

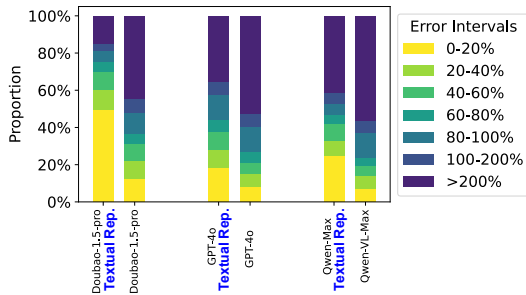


Figure 5: **Textual Input vs. Visual Input** This figure compares the accuracy of two sibling models using textual representation versus 3D spatial representation as input. The three columns correspond to three pairs of sibling LLMs/VLMs. This comparison disentangles high-level reasoning from spatial perception, revealing that existing VLMs struggle to effectively extract spatial information when solving complex visual problems, resulting in low accuracy.

3D scene that reflects its conditions. Using this pipeline, we constructed a dataset of 891 samples for our SIRI-Bench. Although the current dataset is of moderate size, the engine is fully scalable and can support the generation of larger datasets in the future.

3.4 Other Details

Our 3D spatial representations are not directly fed to the tested VLMs. Instead, we capture videos of each scene by orbiting a camera around the main geometric object, and use these videos as the final inputs. Specifically, the camera follows a circular path positioned 8 meters away from the object, with a downward tilt of 30 degrees relative to the horizontal plane. This ensures an appropriate level of visibility. For the indoor envi-

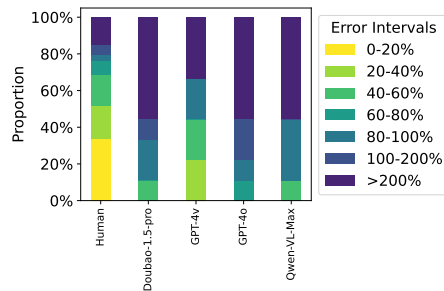


Figure 6: **Comparison with Human Performance.** This figure compares the performance of human participants (the 1st bar) with four state-of-the-art VLM models on a subset of the SIRI-Bench. The results show that current state-of-the-art VLMs are still far from matching human performance.

ronment that serves as the background, we utilize home scenes from the 3D-Front dataset (Fu et al., 2021a,b), which features realistic room layouts and furniture models. Our 3D scenes support highly flexible and customizable rendering setups. Although our SIRI-Bench currently adopts a fixed configuration, parameters such as background layout, lighting, rendering style, camera angle, camera path, and resolution can be adjusted, enabling more diverse evaluation settings in future extensions.

3.5 Data Samples in SIRI-Bench

In fig. 3, we present some illustrative samples from SIRI-Bench, along with their original questions and intermediate steps in the data generation process. More examples can be found in the Supplementary Materials. As can be seen from the original questions compared to the final questions, our data generation engine accurately conceals the mathematical conditions that VLMs need to extract from

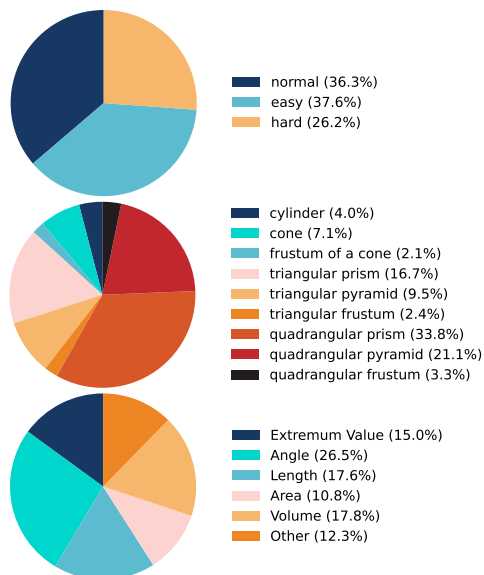


Figure 7: **Data Distribution.** The SIRI-Bench dataset ensures a balanced distribution across difficulty levels (up), geometric types (middle), and problem types (bottom).

the video, while retaining other auxiliary information. Additionally, the engine successfully replaces vertex indices and aligns them accurately with the 3D space.

The intermediate results validate that our engine can correctly solve the dimensions for the geometric entities. Notably, solving geometric conditions for sample #0008 is particularly complicated. Despite that, our math-specialist agent still correctly solves the problem, demonstrating its reliability.

The comparison between the original answers and our final numerical answers demonstrates that our engine can accurately compute the numerical answer for each question while accounting for scaling effects. Overall, the visualized results confirm the reliability of our Automatic Scene Creation Engine, which can generate faithful 3D scenes for any 3D geometry math problem.

3.6 Data Statistics

The dataset of our SIRI-Bench, consists of 891 samples, each formatted as a video-question-answer triplet. The videos are 3 seconds long, recorded at 16 fps with a resolution of 1200×900, and stored in MP4 format. Each question is written in English. The answer is provided as a numerical value, without any symbolic expressions such as square roots or π . All problems are 3D geometry questions, covering nine common types of solids with a balanced distribution across solid types, problem types, and

difficulty levels (shown in fig. 7). Together, these properties make SIRI-Bench a robust and reliable foundation for evaluating spatially grounded reasoning.

4 Experiment

This work aims to evaluate the spatially grounded reasoning capability of current VLMs. In this section, we conduct systematic experiments to assess the performance of existing VLMs on the proposed SIRI-Bench. We present our experimental setup, results, and detailed analysis in the following subsections.

4.1 Experimental Setup

Evaluation Metrics. Our evaluation aims to jointly assess both spatial estimation accuracy and mathematical reasoning correctness. To achieve this, we compute the relative error between the predicted numerical answer and the ground-truth value. The relative error is defined as the absolute difference divided by the ground-truth, expressed as a percentage, which can be expressed as:

$$\frac{|\hat{y} - y|}{y} \times 100\%, \quad (1)$$

where \hat{y} denotes the predicted numerical value and y denotes the ground-truth numerical value. This single metric effectively captures errors arising from either spatial misinterpretation or reasoning mistakes.

To better analyze performance, we categorize the relative error into seven intervals: 0–20%, 20–40%, 40–80%, 80–100%, 100–200%, and $\geq 200\%$. We then examine the distribution of model predictions across these intervals. A strong model is expected to have a distribution concentrated in lower-error intervals, while weaker models show a higher error distribution.

Baselines. We evaluated a variety of state-of-the-art VLMs commonly used in the field. Our selection includes models of different sizes, both open-source models and close-source models, as well as both non-reasoning models and reasoning models (which feature a long reasoning process when solving the problems). Specifically, the models we evaluated include¹:

- OpenAI: GPT-4o (OpenAI, 2024) and GPT-4v (OpenAI, 2023).

¹The specific versions we used is gpt-4o-2024-08-06, gpt-4-turbo-2024-04-09, and qwen-vl-max-2024-11-19

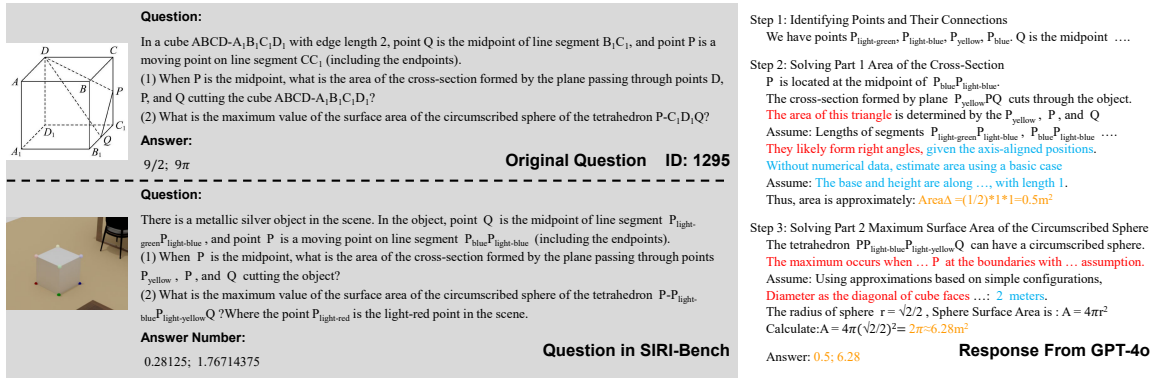


Figure 8: **Display of GPT4o’s Full Answer.** This figure displays the full response from GPT-4o on a case example, with spatial interpretation errors, spatial perception errors, and the final incorrect result highlighted in red, blue, and orange, respectively. The visualization illustrates that GPT4o struggles to extract problem-solving conditions from visual inputs, and tends to make unjustified assumptions that ultimately lead to incorrect answers.

- Qwen-VL: Qwen2-VL-7B (Wang et al., 2024b), Qwen2.5-VL-7B, 32B, 72B (Yang et al., 2024a), QVQ-72B (Team, 2024c), and a close-source model Qwen-VL-Max (Team, 2024d).
- Doubao: Doubao-1.5-pro (Team, 2025a).
- Intern-VL: InternVL2-8B (Team, 2024b), InternVL2.5-8B, 26B, 78B (Chen et al., 2024f).
- LLaVA-Next-Video: LLaVA-NV-7B and 34B (Zhang et al., 2024c).
- Others: SpaceQwen-3B (Chen et al., 2024a), a model fine-tuned for enhancing spatial intelligence.
- LLM: Doubao-1.5-pro (Textual Rep.) (Team, 2025a), which is an LLM that accesses the full mathematical conditions through textual descriptions rather than videos of 3D scenes. We additionally evaluate this method to disentangle high-level reasoning from spatial perception.

4.2 Overall Performance

The overall performance of existing VLMs is summarized in fig. 4, which presents the distribution of prediction errors across seven intervals ranging from 0% to over 200%. A higher concentration of predictions in the lower error intervals indicates greater accuracy.

As shown in the table, all the evaluated VLMs exhibit significantly poor performance on the SIRI-Bench. Specifically, the best-performing method is Doubao-1.5-pro (Team, 2025a). (For Doubao-1.5-pro-Textual-Rep., it is an LLM that inputs textual representation. We do not discuss it in this section and leave it to the section 4.3.) The best-

performing method, Doubao-1.5-pro, has 20% of its predictions within the 0%–40% error range, indicating that it can reasonably estimate the dimensions of the geometric entities and solve the problems for 40% of the cases. This result aligns well with that of other benchmarks, as Doubao-1.5-pro has demonstrated outstanding performance on other multimodal reasoning datasets such as Math-Vision (Wang et al., 2024a) and MathVista (Lu et al., 2023). However, 50% of its predictions have errors exceeding 100%, highlighting its limitations.

Other models perform even worse compared to Doubao-1.5-pro. Specifically, among the open-source models, Qwen2.5-VL-72B shows the best performance, with 50% of its predictions having errors below 100%. However, it fails to achieve higher precision, as only 10% of its predictions have errors below 60%. In the case of close-source models, aside from the best-performing method Doubao-1.5-pro, the other methods achieve similar error distributions, indicating similar performance levels.

It seems that model performance is not obviously influenced by whether the model is open-source or close-source, or by its parameter size. For instance, increasing model size does not necessarily lead to better performance, as the error distributions of InternVL-8B, 26B, 78B are nearly identical. This implies that enhancing the spatially grounded reasoning ability of VLMs may need other strategies beyond simply increasing model size.

Additionally, SpaceQwen-3B (Chen et al., 2024a), a model fine-tuned for spatial intelligence, is particularly noteworthy. Despite its small size, it shows competitive performance, with 25% of its

predictions having errors below 80%. However, its performance remains unsatisfactory. This may be due to its small size and limited fine-tuning, which focuses primarily on the spatial perception rather than the comprehensive spatial reasoning ability.

In summary, existing VLMs fail to solve the problems in the SIRI-Bench dataset effectively. The challenges may stem from two possible factors: (1) These models struggle to estimate the dimensions of the geometric entities, as their specific dimensions are not directly provided in the questions. (2) These models exhibit deficiencies in mathematical reasoning and calculation. Overall, the poor performance across models underscores the significant limitations of current VLMs in spatial reasoning and highlights the value of the SIRI-Bench in identifying these gaps.

4.3 Textual Rep. vs. 3D Spatial Rep.

As shown in fig. 4, the Doubao-1.5-pro-Textual-Rep. method significantly outperforms other VLM methods. This method is an LLM model that uses textual representations as input and accesses full mathematical conditions through text.

To further investigate this phenomenon, we further compare three pairs of sibling models, each consisting of an LLM and a VLM, with nearly identical model properties. The LLMs use text as input, directly extracting key conditions directly from the text (i.e. textual representation). While the VLMs use video as input, they are required to capture problem-solving conditions from the 3D scene depicted in the video (i.e. 3D spatial representation).

Specifically, to maintain consistency with the 3D spatial representation, our textual representation does not use the raw math questions from the original dataset. Instead, we employ the same textual input as the 3D spatial representation, supplemented with dimensional information about the main geometric entities. This ensures that LLMs receive information nearly identical to that of VLMs, with the sole difference being that spatial information is provided in textual form. The results of this comparison are presented in fig. 5. This comparison disentangles high-level reasoning from spatial perception, allowing us to further examine the underlying reason of VLM’s poor performance.

As seen in fig. 5, all three pairs of models exhibit the same trend: the text-input models consistently outperform their video-input counterparts. For example, in terms of prediction error less than 20%,

the proportion nearly doubled when switching from video input to text input, increasing from 12.4%, 8.3%, 7.4% to 49.5%, 18.4%, 27.4%, respectively. Most notably, the Doubao-1.5-pro-Textual-Rep. achieves the most accurate results among all the evaluated models, with about 50% of its predictions having errors below 20% and over 70% of its predictions having errors below 80%. This indicates that while current state-of-the-art models can effectively handle complex reasoning problems based on language, they fail to do the same on the visual level. When solving complex reasoning problems based on visual input, they are unable to effectively extract information, especially the spatial information, from visual modality.

The strong performance of Doubao-1.5-pro also validate the effectiveness of SIRI-Bench, showing that most questions in SIRI-Bench can be correctly solved once provided with full spatial conditions.

Overall, these results underscore the motivation of this paper and highlight the significance of the SIRI-Bench dataset. By challenging VLMs with complex problems that require spatial intelligence, SIRI-Bench reveals the limitations of VLMs in utilizing spatial information for reasoning.

4.4 Comparison with Human Performance

In this part, we investigate how far VLMs are from matching human performance. We randomly select seven samples from the SIRI-Bench dataset and give them to human participants with undergraduate or graduate-level backgrounds. Participants are asked to solve these problems as accurately as possible without any additional information. The average error distributions of human participants is shown in fig. 6, alongside four state-of-the-art VLMs.

As shown in fig. 6, there is a significant gap between the performance of VLMs and human participants. Participants are able to solve over 30% problems with errors within 20%. In contrast, none of the four VLMs achieve this level of accuracy for any of the problems. When allowing for a 60% error margin, participants successfully solve approximately 70% of the problems, a rate far exceeding that of the VLMs.

Notably, some problems are difficult even for human participants, with errors exceeding 100%. This may be due to deviations in human distance estimation, which could accumulate during calculations.

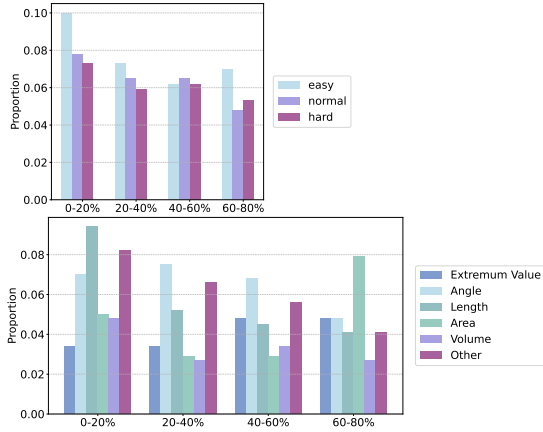


Figure 9: **Error Distribution by Difficulty & Type.** The error distribution of VLMs on our benchmark is shown with respect to question difficulty (top) and question type (bottom). Four error intervals (0–20%, 20–40%, 40–60%, 60–80%) are displayed. The results indicate a relatively balanced failure rate across different difficulty levels and question types.

Overall, the performance of existing state-of-the-art VLMs falls considerably short of human capability, highlighting the substantial limitations in spatial perception and reasoning ability of current VLMs.

4.5 Error Distribution by Difficulty & Type

We assessed the error distributions of VLMs on our complex spatial reasoning benchmark along two dimensions (question difficulty and question type), using four error-rate intervals. Figure 9 (top) illustrates the proportion of items in each interval for three difficulty levels, while figure 9 (bottom) presents analogous data for six question types. The distributions reveal no discernible systematic bias with respect to either difficulty or type, indicating that VLMs exhibit comparable error rates across all questions. This indicates that current VLMs exhibit a relatively uniform failure profile across both difficulty levels and question types, with no evidence of systematic bias.

4.6 Why QVQ Performs So Poorly

As illustrated in Figure 1 of our main paper, QVQ demonstrates the lowest performance among all evaluated VLMs on the SIRI-Bench benchmark. Given QVQ’s design as a multimodal reasoning model with advanced visual understanding capabilities, this underperformance warrants further investigation. Upon examining its reasoning processes, we observe that QVQ often engages in extended

chains of thought, **spanning up to 8K or even 16K tokens, without arriving at a definitive conclusion.** This behavior suggests that QVQ becomes entangled in recursive reasoning loops, failing to produce final answers. Consequently, its responses are categorized as having errors exceeding 200%, contributing to its poor performance metrics.

4.7 Case Study

Figure 8 presents a case study showing the full reasoning process of GPT-4o, with key errors highlighted. Red, blue, and orange marks denote spatial interpretation errors, spatial perception errors, and the final incorrect result, respectively. This case study reveals potential reasons for GPT-4o’s poor performance on SIRI-Bench.

This example involves two sub-questions. The first asks for the area of the cross-section formed by the plane defined by points D, P, and Q intersecting a cube. GPT-4o oversimplifies the geometry by directly treating the cross-section as a triangle DPQ. However, the cross-section is actually a rectangle. Without correctly extracting spatial cues from the video, it further assumes the triangle is right-angled, which is incorrect. It also incorrectly estimates the cube’s size by assuming a unit-length edge, ultimately leading to an incorrect answer.

The second sub-question involves finding an extremum value as the point P moves within the geometry. GPT-4o fails to identify the correct limiting configuration, instead using the cube’s diagonal as a shortcut. Again, it mistakenly estimates the cube’s dimensions and arrives at an incorrect solution.

Overall, this example highlights GPT-4o’s difficulty in interpreting geometric constraints and demonstrates its tendency to make unjustified assumptions when dealing with implicit visual information. Rather than leveraging the video to resolve ambiguity, GPT-4o often proceeds with incomplete reasoning, revealing a key problem-solving limitation in the visual domain.

5 Conclusion

This paper presents SIRI-Bench, a benchmark designed to assess the spatial intelligence of Vision-Language Models (VLMs) through 3D math problems. SIRI-Bench consists of 891 video-question-answer triplets, where each question is formulated within a realistic 3D scene captured in video format. Solving these questions requires models to

extract, interpret, and perform reasoning based on spatial cues, offering a novel and rigorous evaluation of VLMs' spatially grounded reasoning ability. To construct this dataset efficiently, we develop an Automatic Scene Creation Engine that converts abstract math problems into realistic 3D scenes and renders corresponding videos. This engine employs multiple specialized LLM agents within a structured workflow to ensure reliable scene generation while significantly reducing the cost of large-scale data production. Experiments on SIRI-Bench demonstrate that existing VLMs consistently fail to solve more than 50% problems when spatial information must be inferred from video. Their performance not only falls far behind human level but also lags significantly behind their text-only counterparts, which are provided with explicit mathematical conditions in text form. These results indicate that VLMs struggle to extract essential spatial information from visual input for complex reasoning. By posing complex reasoning problems in realistic 3D scenes, SIRI-Bench reveals critical limitations in VLMs' spatially grounded reasoning, which merit further advancement.

References

- Josh Achiam, Steven Adler, Sandhini Agarwal, Lama Ahmad, Ilge Akkaya, Florencia Leoni Aleman, Diogo Almeida, Janko Altenschmidt, Sam Altman, Shyamal Anadkat, et al. 2023. Gpt-4 technical report. *arXiv preprint arXiv:2303.08774*.
- Aida Amini, Saadia Gabriel, Peter Lin, Rik Koncel-Kedziorski, Yejin Choi, and Hannaneh Hajishirzi. 2019. Mathqa: Towards interpretable math word problem solving with operation-based formalisms. *arXiv preprint arXiv:1905.13319*.
- Blender Online Community. 2022. *Blender - a 3D modelling and rendering package*. Blender Foundation, Blender Institute, Amsterdam.
- Anthony Brohan, Noah Brown, Justice Carbajal, Yevgen Chebotar, Xi Chen, Krzysztof Choromanski, Tianli Ding, Danny Driess, Avinava Dubey, Chelsea Finn, et al. 2023. Rt-2: Vision-language-action models transfer web knowledge to robotic control. *arXiv preprint arXiv:2307.15818*.
- Anthony Brohan, Noah Brown, Justice Carbajal, Yevgen Chebotar, Joseph Dabis, Chelsea Finn, Keerthana Gopalakrishnan, Karol Hausman, Alex Herzog, Jasmine Hsu, et al. 2022. Rt-1: Robotics transformer for real-world control at scale. *arXiv preprint arXiv:2212.06817*.
- Keshigeyan Chandrasegaran, Agrim Gupta, Lea M Hadzic, Taran Kota, Jimming He, Cristóbal Eyzaguirre, Zane Durante, Manling Li, Jiajun Wu, and Fei-Fei Li. 2024. Hourvideo: 1-hour video-language understanding. *Advances in Neural Information Processing Systems*, 37:53168–53197.
- Boyuan Chen, Zhuo Xu, Sean Kirmani, Brain Ichter, Dorsa Sadigh, Leonidas Guibas, and Fei Xia. 2024a. Spatialvlm: Endowing vision-language models with spatial reasoning capabilities. In *Proceedings of the IEEE/CVF Conference on Computer Vision and Pattern Recognition*, pages 14455–14465.
- Jiaqi Chen, Jianheng Tang, Jinghui Qin, Xiaodan Liang, Lingbo Liu, Eric P Xing, and Liang Lin. 2021a. Geoqa: A geometric question answering benchmark towards multimodal numerical reasoning. *arXiv preprint arXiv:2105.14517*.
- Junying Chen, Zhenyang Cai, Ke Ji, Xidong Wang, Wanlong Liu, Rongsheng Wang, Jianye Hou, and Benyou Wang. 2024b. Huatuoqpt-o1, towards medical complex reasoning with llms. *arXiv preprint arXiv:2412.18925*.
- Junying Chen, Chi Gui, Anningzhe Gao, Ke Ji, Xidong Wang, Xiang Wan, and Benyou Wang. 2024c. Cod, towards an interpretable medical agent using chain of diagnosis. *arXiv preprint arXiv:2407.13301*.
- Kehua Chen, Zhenlong Yuan, Tianlu Mao, and Zhaoqi Wang. 2024d. Dual-Level Precision Edges Guided Multi-View Stereo with Accurate Planarization. In *Proceedings of the AAAI Conference on Artificial Intelligence*, volume 39, pages 2105–2113.
- Lin Chen, Jinsong Li, Xiaoyi Dong, Pan Zhang, Yuhang Zang, Zehui Chen, Haodong Duan, Jiaqi Wang, Yu Qiao, Dahua Lin, et al. 2024e. Are we on the right way for evaluating large vision-language models? *arXiv preprint arXiv:2403.20330*.
- Mark Chen, Jerry Tworek, Heewoo Jun, Qiming Yuan, Henrique Ponde De Oliveira Pinto, Jared Kaplan, Harri Edwards, Yuri Burda, Nicholas Joseph, Greg Brockman, et al. 2021b. Evaluating large language models trained on code. *arXiv preprint arXiv:2107.03374*.
- Zhe Chen, Weiyun Wang, Yue Cao, Yangzhou Liu, Zhangwei Gao, Erfei Cui, Jinguo Zhu, Shenglong Ye, Hao Tian, Zhaoyang Liu, et al. 2024f. Expanding performance boundaries of open-source multimodal models with model, data, and test-time scaling. *arXiv preprint arXiv:2412.05271*.
- Yew Ken Chia, Vernon Toh Yan Han, Deepanway Ghosal, Lidong Bing, and Soujanya Poria. 2024. Puzzlevqa: Diagnosing multimodal reasoning challenges of language models with abstract visual patterns. *arXiv preprint arXiv:2403.13315*.
- Andrew J Davison. 2018. Futuremapping: The computational structure of spatial ai systems. *arXiv preprint arXiv:1803.11288*.
- Danny Driess, Fei Xia, Mehdi S. M. Sajjadi, Corey Lynch, Aakanksha Chowdhery, Brian Ichter, Ayzaan Wahid, Jonathan Tompson, Quan Vuong, Tianhe Yu, Wenlong Huang, Yevgen Chebotar, Pierre Sermanet, Daniel Duckworth, Sergey Levine, Vincent Vanhoucke, Karol Hausman, Marc Toussaint, Klaus Greff, Andy Zeng, Igor Mordatch, and Pete Florence. 2023. *Palm-e: An embodied multimodal language model*.
- Sinan Fan, Liang Xie, Chen Shen, Ge Teng, Xiaosong Yuan, Xiaofeng Zhang, Chenxi Huang, Wenxiao Wang, Xiaofei He, and Jieping Ye. 2025. Improving complex reasoning with dynamic prompt corruption: A soft prompt optimization approach. *arXiv preprint arXiv:2503.13208*.
- Huan Fu, Bowen Cai, Lin Gao, Ling-Xiao Zhang, Jiaming Wang, Cao Li, Qixun Zeng, Chengyue Sun, Rongfei Jia, Binqiang Zhao, et al. 2021a. 3d-front: 3d furnished rooms with layouts and semantics. In *Proceedings of the IEEE/CVF International Conference on Computer Vision*, pages 10933–10942.
- Huan Fu, Rongfei Jia, Lin Gao, Mingming Gong, Binqiang Zhao, Steve Maybank, and Dacheng Tao. 2021b. 3d-future: 3d furniture shape with texture. *International Journal of Computer Vision*, pages 1–25.
- Xingyu Fu, Yushi Hu, Bangzheng Li, Yu Feng, Haoyu Wang, Xudong Lin, Dan Roth, Noah A Smith, Wei-Chiu Ma, and Ranjay Krishna. 2024. Blink: Multimodal large language models can see but not perceive.

- In *European Conference on Computer Vision*, pages 148–166. Springer.
- Howard E Gardner. 2011. *Frames of mind: The theory of multiple intelligences*. Basic books.
- Deepanway Ghosal, Vernon Toh Yan Han, Chia Yew Ken, and Soujanya Poria. 2024. Are language models puzzle prodigies? algorithmic puzzles unveil serious challenges in multimodal reasoning. *arXiv preprint arXiv:2403.03864*.
- Yash Goyal, Tejas Khot, Douglas Summers-Stay, Dhruv Batra, and Devi Parikh. 2017. Making the v in vqa matter: Elevating the role of image understanding in visual question answering. In *Proceedings of the IEEE conference on computer vision and pattern recognition*, pages 6904–6913.
- Kristen Grauman, Andrew Westbury, Eugene Byrne, Zachary Chavis, Antonino Furnari, Rohit Girdhar, Jackson Hamburger, Hao Jiang, Miao Liu, Xingyu Liu, et al. 2022. Ego4d: Around the world in 3,000 hours of egocentric video. In *Proceedings of the IEEE/CVF conference on computer vision and pattern recognition*, pages 18995–19012.
- Daya Guo, Dejian Yang, Haowei Zhang, Junxiao Song, Ruoyu Zhang, Runxin Xu, Qihao Zhu, Shirong Ma, Peiyi Wang, Xiao Bi, et al. 2025. Deepseek-r1: Incentivizing reasoning capability in llms via reinforcement learning. *arXiv preprint arXiv:2501.12948*.
- Dan Hendrycks, Collin Burns, Saurav Kadavath, Akul Arora, Steven Basart, Eric Tang, Dawn Song, and Jacob Steinhardt. 2021. Measuring mathematical problem solving with the math dataset. *arXiv preprint arXiv:2103.03874*.
- Sirui Hong, Xiawu Zheng, Jonathan Chen, Yuheng Cheng, Jinlin Wang, Ceyao Zhang, Zili Wang, Steven Ka Shing Yau, Zijuan Lin, Liyang Zhou, et al. 2023. Metagpt: Meta programming for multi-agent collaborative framework. *arXiv preprint arXiv:2308.00352*.
- Drew A Hudson and Christopher D Manning. 2019. Gqa: A new dataset for real-world visual reasoning and compositional question answering. In *Proceedings of the IEEE/CVF conference on computer vision and pattern recognition*, pages 6700–6709.
- Aaron Jaech, Adam Kalai, Adam Lerer, Adam Richardson, Ahmed El-Kishky, Aiden Low, Alec Helyar, Aleksander Madry, Alex Beutel, Alex Carney, et al. 2024. Openai o1 system card. *arXiv preprint arXiv:2412.16720*.
- Justin Johnson, Bharath Hariharan, Laurens Van Der Maaten, Li Fei-Fei, C Lawrence Zitnick, and Ross Girshick. 2017. Clevr: A diagnostic dataset for compositional language and elementary visual reasoning. In *Proceedings of the IEEE conference on computer vision and pattern recognition*, pages 2901–2910.
- Aitor Lewkowycz, Anders Andreassen, David Dohan, Ethan Dyer, Henryk Michalewski, Vinay Ramasesh, Ambrose Slone, Cem Anil, Imanol Schlag, Theo Gutman-Solo, et al. 2022. Solving quantitative reasoning problems with language models. *Advances in Neural Information Processing Systems*, 35:3843–3857.
- Rong Li, Shijie Li, Lingdong Kong, Xulei Yang, and Junwei Liang. 2024. Seeground: See and ground for zero-shot open-vocabulary 3d visual grounding. *arXiv preprint arXiv:2412.04383*.
- Yujia Li, David Choi, Junyoung Chung, Nate Kushman, Julian Schrittwieser, Rémi Leblond, Tom Eccles, James Keeling, Felix Gimeno, Agustin Dal Lago, et al. 2022. Competition-level code generation with alphacode. *Science*, 378(6624):1092–1097.
- Hunter Lightman, Vineet Kosaraju, Yura Burda, Harri Edwards, Bowen Baker, Teddy Lee, Jan Leike, John Schulman, Ilya Sutskever, and Karl Cobbe. 2023. Let’s verify step by step. *arXiv preprint arXiv:2305.20050*.
- Bin Lin, Yang Ye, Bin Zhu, Jiayi Cui, Munan Ning, Peng Jin, and Li Yuan. 2023. Video-llava: Learning united visual representation by alignment before projection. *arXiv preprint arXiv:2311.10122*.
- Cong Liu, Zhenlong Yuan, You Wang, Yanhua Yin, Weichao Luo, Zhenyu He, and Xiaojun Liang. 2025. MR-IntelliAssist: A World Cognition Agent Enabling Adaptive Human-AI Symbiosis in Industry 4.0. In Helmut Degen and Stavroula Ntoa, editors, *Artificial Intelligence in HCI*, volume 15822, pages 163–177. Springer Nature Switzerland.
- Yuan Liu, Haodong Duan, Yuanhan Zhang, Bo Li, Songyang Zhang, Wangbo Zhao, Yike Yuan, Jiaqi Wang, Conghui He, Ziwei Liu, et al. 2024. Mmbench: Is your multi-modal model an all-around player? In *European conference on computer vision*, pages 216–233. Springer.
- Pan Lu, Hritik Bansal, Tony Xia, Jiacheng Liu, Chunyuan Li, Hannaneh Hajishirzi, Hao Cheng, Kai-Wei Chang, Michel Galley, and Jianfeng Gao. 2023. Mathvista: Evaluating mathematical reasoning of foundation models in visual contexts. *arXiv preprint arXiv:2310.02255*.
- Pan Lu, Bowen Chen, Sheng Liu, Rahul Thapa, Joseph Boen, and James Zou. 2025. Octotools: An agentic framework with extensible tools for complex reasoning. *arXiv preprint arXiv:2502.11271*.
- Muhammad Maaz, Hanoona Rasheed, Salman Khan, and Fahad Shahbaz Khan. 2023. Video-chatgpt: Towards detailed video understanding via large vision and language models. *arXiv preprint arXiv:2306.05424*.
- Mikołaj Małkiński, Szymon Pawlonka, and Jacek Mańdziuk. 2024. Reasoning limitations of multi-modal large language models. a case study of bongard problems. *arXiv preprint arXiv:2411.01173*.

- Yunze Man, Liang-Yan Gui, and Yu-Xiong Wang. 2024. Situational awareness matters in 3d vision language reasoning. In *Proceedings of the IEEE/CVF Conference on Computer Vision and Pattern Recognition*, pages 13678–13688.
- Karttikeya Mangalam, Raiymbek Akshulakov, and Jitendra Malik. 2023. Egoschema: A diagnostic benchmark for very long-form video language understanding. *Advances in Neural Information Processing Systems*, 36:46212–46244.
- Yongsen Mao, Junhao Zhong, Chuan Fang, Jia Zheng, Rui Tang, Hao Zhu, Ping Tan, and Zihan Zhou. 2025. [Spatiallm: Training large language models for structured indoor modeling](#).
- OpenAI. 2023. Gpt-4v(ision) system card. <https://openai.com/index/gpt-4v-system-card/>.
- OpenAI. 2024. Gpt-4o system card. <https://openai.com/index/gpt-4o-system-card/>.
- Abby O’Neill, Abdul Rehman, Abhiram Maddukuri, Abhishek Gupta, Abhishek Padalkar, Abraham Lee, Acorn Pooley, Agrim Gupta, Ajay Mandlekar, Ajinkya Jain, et al. 2024. Open x-embodiment: Robotic learning datasets and rt-x models: Open x-embodiment collaboration 0. In *2024 IEEE International Conference on Robotics and Automation (ICRA)*, pages 6892–6903. IEEE.
- Khaled Saab, Tao Tu, Wei-Hung Weng, Ryutaro Tanno, David Stutz, Ellery Wulczyn, Fan Zhang, Tim Strother, Chunjong Park, Elahe Vedadi, et al. 2024. Capabilities of gemini models in medicine. *arXiv preprint arXiv:2404.18416*.
- DeepMind Team. 2024a. Genie 2: A large-scale foundation world model. <https://deepmind.google/discover/blog/genie-2-a-large-scale-foundation-world-model>.
- DouBao Team. 2025a. Doubao-1.5-pro. https://team.doubao.com/zh/special/doubao_1_5_pro.
- OpenGVLab Team. 2024b. Internv12: Better than the best—expanding performance boundaries of open-source multimodal models with the progressive scaling strategy. <https://internvl.github.io/blog/2024-07-02-InternVL-2.0/>.
- Qwen Team. 2024c. [Qvq: To see the world with wisdom](#).
- Qwen Team. 2024d. Qwen-vl-max. <https://huggingface.co/spaces/Qwen/Qwen-VL-Max>.
- Qwen Team. 2025b. [Qwq-32b: Embracing the power of reinforcement learning](#).
- WorldLabs Team. 2024e. World labs :generating world. <https://www.worldlabs.ai/>.
- the University of Utah. 2024. 22nd international conference on artificial intelligence in medicine. <https://aime24.aimeicine.info/>.
- Ke Wang, Juntong Pan, Weikang Shi, Zimu Lu, Houxing Ren, Aojun Zhou, Mingjie Zhan, and Hongsheng Li. 2024a. Measuring multimodal mathematical reasoning with math-vision dataset. *Advances in Neural Information Processing Systems*, 37:95095–95169.
- Peng Wang, Shuai Bai, Sinan Tan, Shijie Wang, Zhihao Fan, Jinze Bai, Keqin Chen, Xuejing Liu, Jialin Wang, Wenbin Ge, et al. 2024b. Qwen2-vl: Enhancing vision-language model’s perception of the world at any resolution. *arXiv preprint arXiv:2409.12191*.
- Jason Wei, Xuezhi Wang, Dale Schuurmans, Maarten Bosma, Fei Xia, Ed Chi, Quoc V Le, Denny Zhou, et al. 2022. Chain-of-thought prompting elicits reasoning in large language models. *Advances in neural information processing systems*, 35:24824–24837.
- Yuxi Wei, Zi Wang, Yifan Lu, Chenxin Xu, Changxing Liu, Hao Zhao, Siheng Chen, and Yanfeng Wang. 2024. Editable scene simulation for autonomous driving via collaborative llm-agents. In *Proceedings of the IEEE/CVF Conference on Computer Vision and Pattern Recognition*, pages 15077–15087.
- Qingyun Wu, Gagan Bansal, Jieyu Zhang, Yiran Wu, Shaokun Zhang, Erkang Zhu, Beibin Li, Li Jiang, Xiaoyun Zhang, and Chi Wang. 2023. Auto-gen: Enabling next-gen llm applications via multi-agent conversation framework. *arXiv preprint arXiv:2308.08155*.
- An Yang, Baosong Yang, Beichen Zhang, Binyuan Hui, Bo Zheng, Bowen Yu, Chengyuan Li, Dayiheng Liu, Fei Huang, Haoran Wei, Huan Lin, Jian Yang, Jianhong Tu, Jianwei Zhang, Jianxin Yang, Jiayi Yang, Jingren Zhou, Junyang Lin, Kai Dang, Keming Lu, Keqin Bao, Kexin Yang, Le Yu, Mei Li, Mingfeng Xue, Pei Zhang, Qin Zhu, Rui Men, Runji Lin, Tianhao Li, Tianyi Tang, Tingyu Xia, Xingzhang Ren, Xuancheng Ren, Yang Fan, Yang Su, Yichang Zhang, Yu Wan, Yuqiong Liu, Zeyu Cui, Zhenru Zhang, and Zihan Qiu. 2024a. Qwen2.5 technical report. *arXiv preprint arXiv:2412.15115*.
- Jihan Yang, Shusheng Yang, Anjali W Gupta, Rilyn Han, Li Fei-Fei, and Saining Xie. 2024b. Thinking in space: How multimodal large language models see, remember, and recall spaces. *arXiv preprint arXiv:2412.14171*.
- Yijun Yang, Tianyi Zhou, Kanxue Li, Dapeng Tao, Lu-song Li, Li Shen, Xiaodong He, Jing Jiang, and Yuhui Shi. 2024c. Embodied multi-modal agent trained by an llm from a parallel textworld. In *Proceedings of the IEEE/CVF Conference on Computer Vision and Pattern Recognition*, pages 26275–26285.
- Yangyang Yu, Zhiyuan Yao, Haohang Li, Zhiyang Deng, Yuechen Jiang, Yupeng Cao, Zhi Chen, Jordan Szechow, Zhenyu Cui, Rong Liu, et al. 2025. Fincon: A

- synthesized llm multi-agent system with conceptual verbal reinforcement for enhanced financial decision making. *Advances in Neural Information Processing Systems*, 37:137010–137045.
- Zhenlong Yuan, Jiakai Cao, Zhaoxin Li, Hao Jiang, and Zhaoqi Wang. 2024a. SD-MVS: Segmentation-Driven Deformation Multi-View Stereo with Spherical Refinement and EM Optimization. In *Proceedings of the AAAI Conference on Artificial Intelligence*, volume 38, pages 6871–6880.
- Zhenlong Yuan, Jiakai Cao, Zhaoqi Wang, and Zhaoxin Li. 2024b. Tsar-mvs: Textureless-aware segmentation and correlative refinement guided multi-view stereo. *Pattern Recognition*, 154:110565.
- Zhenlong Yuan, Cong Liu, Fei Shen, Zhaoxin Li, Jinguo Luo, Tianlu Mao, and Zhaoqi Wang. 2025a. MSP-MVS: Multi-granularity segmentation prior guided multi-view stereo. In *Proceedings of the AAAI Conference on Artificial Intelligence*, volume 39, pages 9753–9762.
- Zhenlong Yuan, Jinguo Luo, Fei Shen, Zhaoxin Li, Cong Liu, Tianlu Mao, and Zhaoqi Wang. 2025b. DVP-MVS: Synergize depth-edge and visibility prior for multi-view stereo. In *Proceedings of the AAAI Conference on Artificial Intelligence*, volume 39, pages 9743–9752.
- Zhenlong Yuan, Zhidong Yang, Yujun Cai, Kuangxin Wu, Mufan Liu, Dapeng Zhang, Hao Jiang, Zhaoxin Li, and Zhaoqi Wang. 2025c. SED-MVS: Segmentation-Driven and Edge-Aligned Deformation Multi-View Stereo with Depth Restoration and Occlusion Constraint. *IEEE Transactions on Circuits and Systems for Video Technology*.
- Xiang Yue, Yuansheng Ni, Kai Zhang, Tianyu Zheng, Ruoqi Liu, Ge Zhang, Samuel Stevens, Dongfu Jiang, Weiming Ren, Yuxuan Sun, et al. 2024. Mmmu: A massive multi-discipline multimodal understanding and reasoning benchmark for expert agi. In *Proceedings of the IEEE/CVF Conference on Computer Vision and Pattern Recognition*, pages 9556–9567.
- Shangjin Zhai, Zhichao Ye, Jialin Liu, Weijian Xie, Jiaqi Hu, Zhen Peng, Hua Xue, Danpeng Chen, Xiaomeng Wang, Lei Yang, et al. 2025. Stargen: A spatiotemporal autoregression framework with video diffusion model for scalable and controllable scene generation. *arXiv preprint arXiv:2501.05763*.
- Jiaxin Zhang, Zhongzhi Li, Mingliang Zhang, Fei Yin, Chenglin Liu, and Yashar Moshfeghi. 2024a. Geoval: benchmark for evaluating llms and multi-modal models on geometry problem-solving. *arXiv preprint arXiv:2402.10104*.
- Renrui Zhang, Dongzhi Jiang, Yichi Zhang, Haokun Lin, Ziyu Guo, Pengshuo Qiu, Aojun Zhou, Pan Lu, Kai-Wei Chang, Yu Qiao, et al. 2024b. Mathverse: Does your multi-modal llm truly see the diagrams in visual math problems? In *European Conference on Computer Vision*, pages 169–186. Springer.
- Yuanhan Zhang, Bo Li, haotian Liu, Yong jae Lee, Liangke Gui, Di Fu, Jiashi Feng, Ziwei Liu, and Chunyuan Li. 2024c. Llava-next: A strong zero-shot video understanding model.